**Pakistan Journal of Engineering and Technology, PakJET**
ISSN (p): 2664-2042, ISSN (e): 2664-2050
Volume: 5, Number: 2, Pages: 204- 210, Year: 2022

# MSP Patches Based Optimized EEG Source Localization and Validation in Visual Cortex of Human Brain

Anwar Ali Gaho[1], Ahmed Muddassir Khan[1], Sayed Hyder Abbas Musavi[2], Muhammad Abul Hasan[3], and Muhammad Shafiq[4]

[1]Department of Electrical Engineering, Faculty of Engineering Science & Technology, Indus University, Karachi, Pakistan
[2]Department of Electronic Engineering, Mehran University of Engineering and Technology, SZAB Khairpur, Pakistan
[3]Department of Biomedical Engineering, NED University of Engineering & Technology, Karachi, Pakistan
[4]University of Innsbruck, Institute for Meteorology Department of Geophysics, Austria

Corresponding author: Anwar Ali Gaho (e-mail: anwar.a.gaho@gmail.com).

**Received: 15/05/2022, Revised: 28/08/2022, Accepted: 15/09/2022**

*Abstract-* **This paper is focused on optimizing EEG source localization of visual neural activities generated in the posterior lobe of the human brain. The visual and neural systems of the human brain process the captured images of faces or scenes into optical and chemical neurons in order to produce electrical potentials over the scalp surface, where EEG electrodes measure these signals to sense the underneath visual brain activity. However, it is categorically hard to localize the true neural sources in the human brain's visual cortex due to overlapping and interaction of other active areas of the lobes of the brain. Thus, a novel algorithm of MSP inversion-based Bayesian framework with varying patches for providing the optimal free energy and minimum location in the visual cortex is proposed to address this issue. This algorithm is integrated with a synthetic EEG dataset generation scheme to validate active neural sources. This proposed algorithm provides satisfactory results in terms of optimal free energy with minimum localization error and validates true active sources in the brain. The SPM12 Toolbox is applied in processing the visual EEG dataset in this research. The application of this proposed algorithm is beneficial in terms of localizing the optimum visual sources and identifying the visual disorders or diseases in the human brain.**

*Index Terms--* **EEG, Free Energy, Inversion, Multiple Sparse Priors, Patches, Synthetic EEG dataset, Validation**

## I. INTRODUCTION

The human brain is a complex organ of the human body due to its cognitive, psychological and functional behaviour [1, 2]. It comprises billions of neurons, forming a group of dipoles on source activation [3]. These neural sources can either be localized or mapped by electroencephalography (EEG). Magnetoencephalography (MEG), functional magnetic resonance imaging (fMRI), near-infrared spectroscopy (NIRS) and electrocorticography (ECoG) techniques [4-5]. In EEG, the neural responses generate event-related potentials (ERPs) on the scalp surface, measured by EEG multi-channel system composed of electrodes, amplifiers, digitizers and filters [6-9]. EEG is preferred due to its low cost and high temporal resolution [10-13]. Since it is hard to localize the actual neural sources underneath due to unwanted noises, experimental limitations and overlapping of neural activities of other lobes of the brain [14-17]. To address this issue, a novel MSP inversion-based Bayesian framework algorithm with irregular patches that give the optimal free energy and minimum location in the visual cortex is proposed to solve EEG ill-posed inverse problems [18, 19]. Since eyes are interlinked with the visual cortex through optical nerves for generating electrical signals in the cortex [20-24], these energized neural sources are explored by varying the patches and validated by a synthetic EEG data scheme. In this paper, Matlab's GUI of statistical parametric mapping (SPM12) toolbox is applied for preprocessing, execution and statistical analysis.

This paper is composed of 6 x sections. Section I covers the introduction. Section II is about the mathematical background. Section III comprises MSP inversion-based Bayesian framework. Section IV is about methodology. Section V and VI cover results and discussion, and conclusion, respectively.

## II. MATHEMATICAL BACKGROUND

The MSP inversion approach based Bayesian framework is stochastic in nature, estimates neural responses for ill-posed inverse problems, and depends upon covariance matrices at both source and sensor levels. This involves parametric empirical Bayes, hyperparameters and variances. The current density and sensors relationship is shown by General Linear Model (GLM) i.e.

$$Y = LJ + \in \tag{1}$$

where $Y \in \mathbb{R}^{N_c N_n}$ represents EEG dataset of $N_c$ sensors and $N_n$ time samples. $L$ is lead field matrix. $J \in \mathbb{R}^{N_d N_n}$ represents a current density of dipoles. $\in$ indicates random noise and uncertainty. Bayes' theorem is given as under:

$$P(J/Y) = \frac{P(Y/J)P(J)}{P(Y)} \tag{2}$$

where $P(J/Y)$ is posterior probability of source estimation. $P(Y/J)$ is likelihood probability of a given source activity. $P(J)$ is prior probability of source activity. $P(Y)$ is constant probability of dataset. The magnitude of current dipoles is estimated by applying expectation operator on $P(J/Y)$ to get estimated current density $\hat{J}$ .

$$\hat{J} = E\left[P(J/Y)\right] \tag{3}$$

The equivalent current density $\hat{J}$ form can be represented by:

$$\hat{J} = QL^T\left(\Sigma_\in + LQL^T\right)^{-1} Y \tag{4}$$

$$F = \log p(Y) \tag{5}$$

The optimization of MSP based Bayesian framework depends upon the optimal value of Free energy ($F$).

$$F = \int q(h)\log p(Y,h)dh - \int q(h)\log q(h)dh \tag{6}$$

$$F = \Psi(Y,h) + \mathrm{H}(h) \tag{7}$$

Free energy involves two parameters expected energy $\Psi(Y,h)$ and entropy $\mathrm{H}(h)$. The gradients for entropy are zero for maximum performance, when computed through Hessian algorithm.

$$H_{i,j} = \frac{\partial^2 \hat{U}(Y,h)}{\partial h_i \partial h_j} \tag{8}$$

So, expected energy can be estimated from:

$$\hat{\Psi} = \int q(h)\hat{U}(Y,h)dh \tag{9}$$

After solving the intermediate steps of expected energy and entropy, FE function called cost function can be represented as:

$$\begin{aligned} F = & -\frac{N_t}{2} tr\left(C_Y \Sigma_Y^{-1}\right) - \frac{N_t}{2}\log\left|\Sigma_Y\right| - \frac{N_t N_n}{2}\log(2\pi)\ldots \\ & -\frac{1}{2} tr\left((\hat{h}-v)^T \Pi(\hat{h}-v)\right) + \frac{1}{2}\log\left|\Sigma_h \Pi\right| \end{aligned} \tag{10}$$

Free energy having no units is expressed in a negative sign called negative free energy.

## III. PROPOSED MSP INVERSION-BASED BAYESIAN FRAMEWORK ALGORITHM

The proposed advanced MSP algorithm with varying patches provides the most optimized FE and minimum localization errors at active neural sources of the brain. The demonstrated results of FE and MNI coordinates of sources are analyzed and validated through a synthetic EEG scheme. The details of the proposed algorithm are shown in Fig 1. This involves forward problem, stimuli of faces, MSP inversion, patches variation, head structures, and synthetic EEG dataset generation with noises and frequencies and iterations.

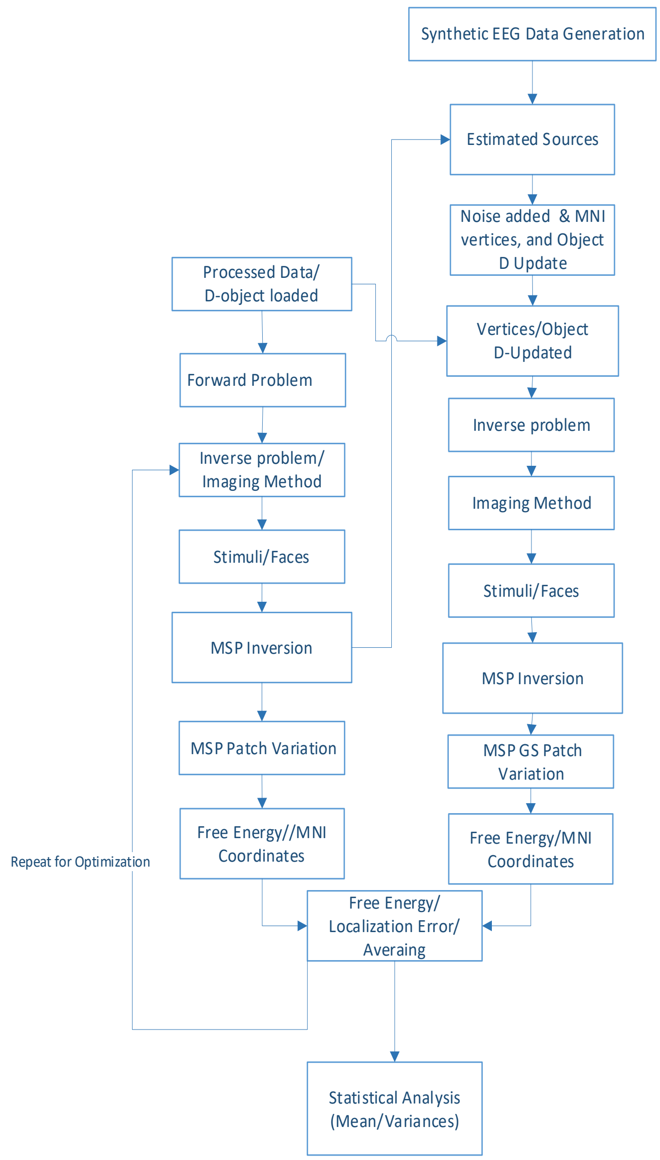


FIGURE 1. Proposed advanced MSP algorithm

## IV. METHODOLOGY

### A. EXPERIMENTATION

EEG dataset was recorded at 1100 Hz from 16 x healthy male and female subjects at the medical research council of cognition and brain sciences unit of Cambridge university [25]. Faces as grey

image stimuli, including famous, familiar and unfamiliar of different ages, expressions, hairstyles and orientations, were displayed on the screen at 1.3 m and were shown to participants for recording visual EEG dataset. The experiment was conducted after the consent of participants and approval of the university. The timeline for experimenting was designed as shown in Fig 2. The circle (o) and crosshair (+) signs were paced for 1700 ms–4256 ms and 400 ms - 600 ms, respectively.
Similarly, stimuli time for faces was fixed for 800 ms - 600 ms. EEG dataset of subjects was saved in D object. In this paper, EEG dataset of 3 x participants, including 2 x females and 1 x male of age of 26, 24 and 30 years, was processed.

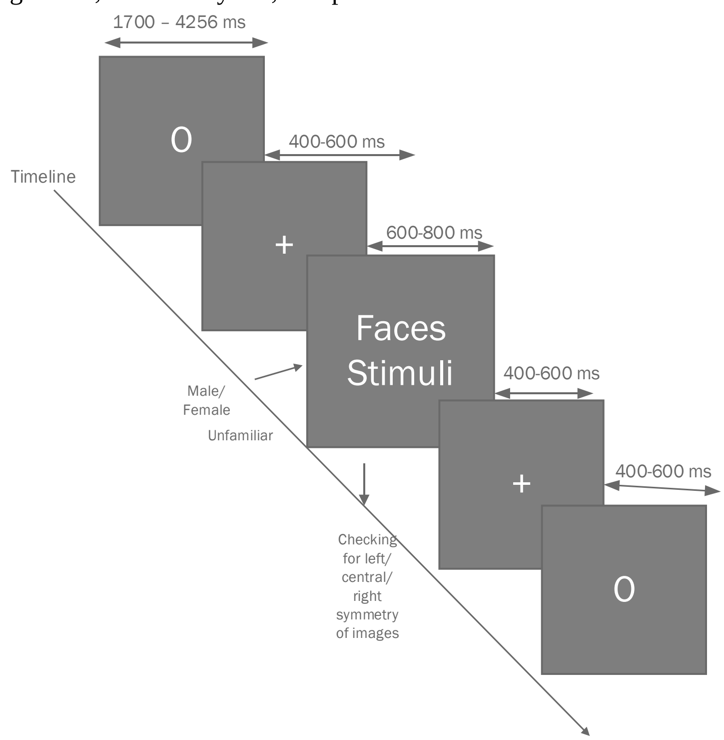


FIGURE 2. Designed timeline for experiment

### B. MSP INVERSION AND STIMULI FACES

MSP inversion is primarily applied for processing EEG datasets. Initially, 256 patches are used to compute FE in Montreal Neurological Institute (MNI) coordinates systems by using a real EEG dataset for generating real reference and its validation through synthetic EEG datasets such as [-38, -65, -13] is created for Subj # 1. The same process is repeated for subj # 2 and subj # 3 to compute the MNI coordinates. The neural projections are displayed in brain glass view images. This practice is repeated 22 x times by varying patches from 350 to 3500 to explore optimized FE at given MNI coordinates for neural sources.

### C. SYNTHETIC EEG DATASET GENERATION

Synthetic EEG data is applied to provide an ideal reference for validating real EEG source localizations and for computing localization error in the visual cortex. A simulated EEG dataset replaces the new D object with the same number of sensors, channels and head positions . This synthetic scheme comprises several steps such as loading simulated EEG dataset, generation of neural sources activity at the evoked locations, noise addition, formation of lead field matrix (L), application of green function for smoothing sources, and addition of white noises and dipole frequencies.

## V. RESULTS AND DISCUSSION

### A. SYNTHETIC EEG DATASET

2 x dipoles of 25 Hz and 15 Hz with neural activity are observed at 4661 and 641 positions in the cortex as shown in Fig 3. These positions are equivalent to [-38, -65, -13] and [36, -66, -12] in MNI coordinates. 8196 x dipoles are located in both left and right hemispheres. Among these, 256 dipoles are located in visual cortex as shown in Fig 4.

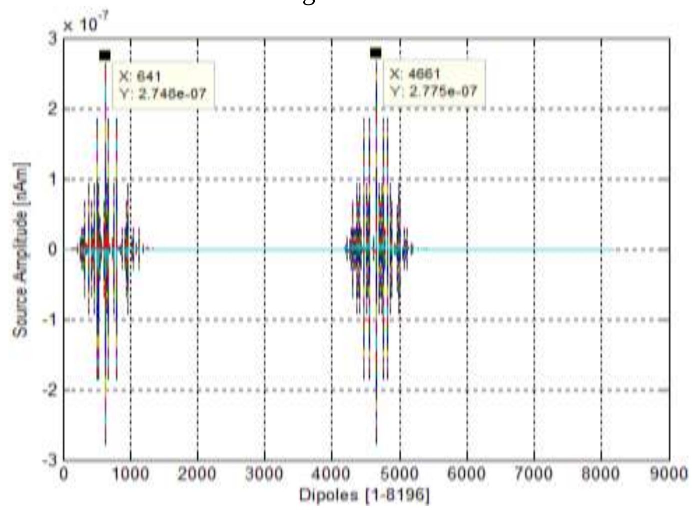


FIGURE 3. Neural activities at 641 and 4661 spaces

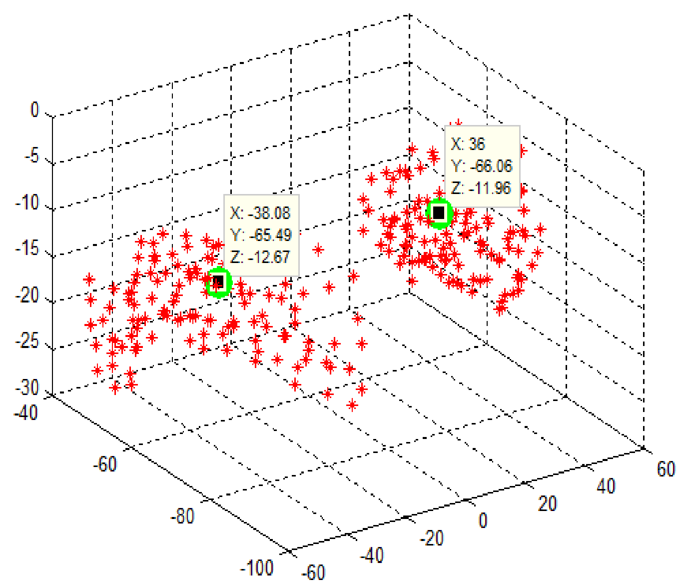


FIGURE 4. Two highlighted sources at MNI Coordinates

The neural map projections at these [-38, -65, -13] and [36, -66, -12] coordinates in the brain glass view are shown in Fig 5. No noise or fake projection can be seen. Only ideal active sources can be observed.

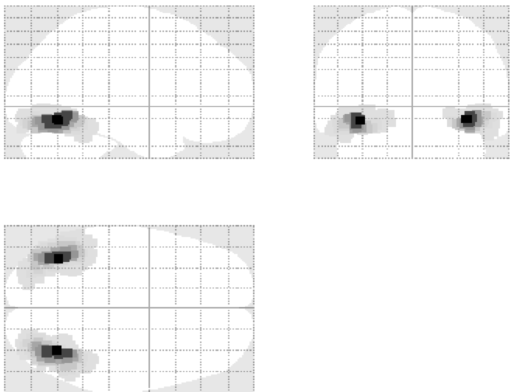

FIGURE 5. Axial, sagittal and coronal projections

B. EEG DATSET

Scalp map of real EEG datasets of 3 x stimuli faces for three subjects are shown in Fig 6 to Fig 8. EEG electrodes measure these scalp signals.

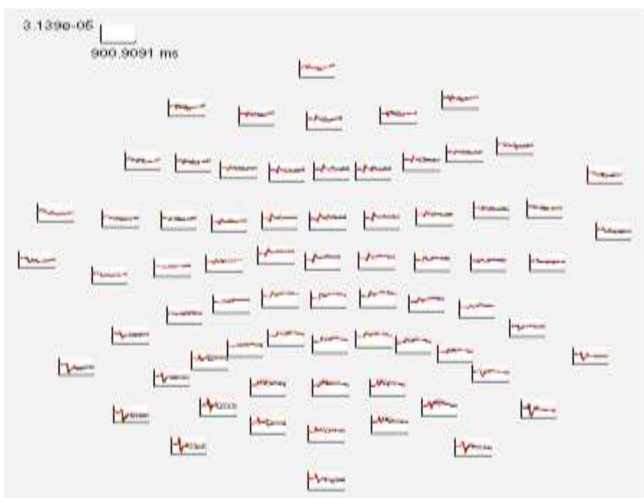


FIGURE 6. Subj # 1: EEG scalp

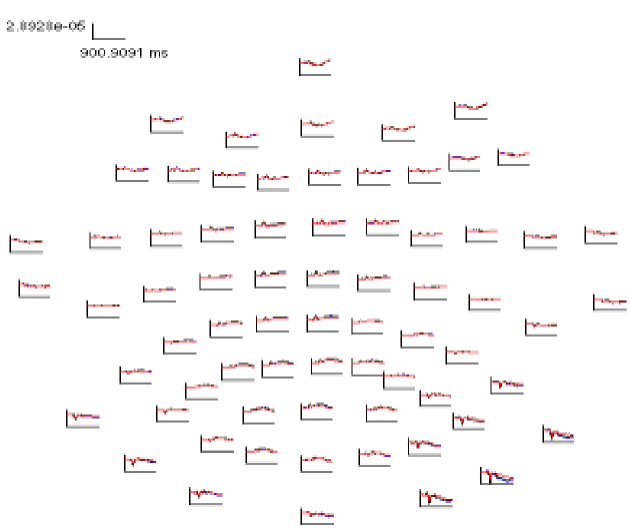


FIGURE 7. Subj # 2: EEG scalp

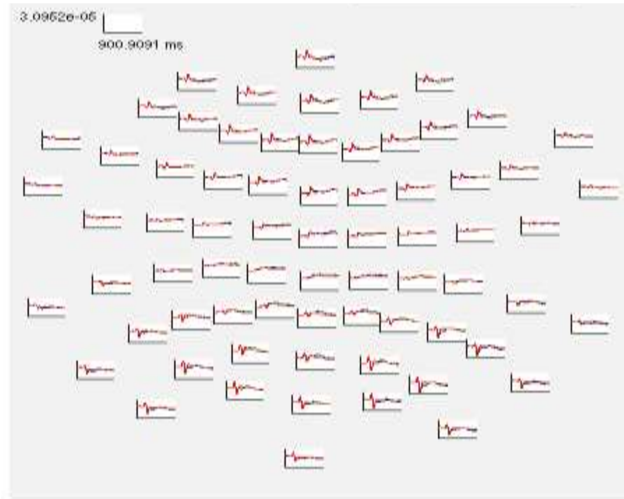


FIGURE 8. Subj # 3: EEG scalp

Channel # 66, comprising of three faces including famous, unfamiliar and scrambled faces of 3 x subjects, are plotted in Fig 9 to Fig 11 to highlight the scalp underneath neural activities.

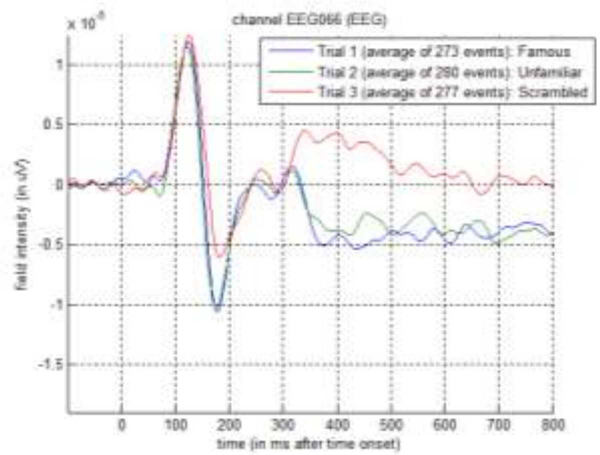


FIGURE 9. Subj # 1: channel # 66

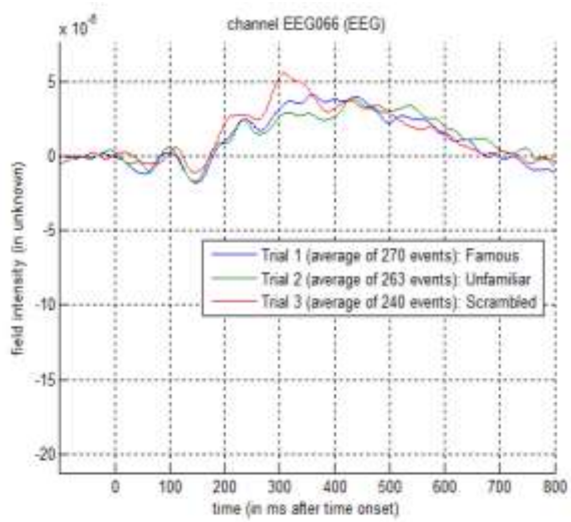


FIGURE 10. Subj # 2: channel # 66

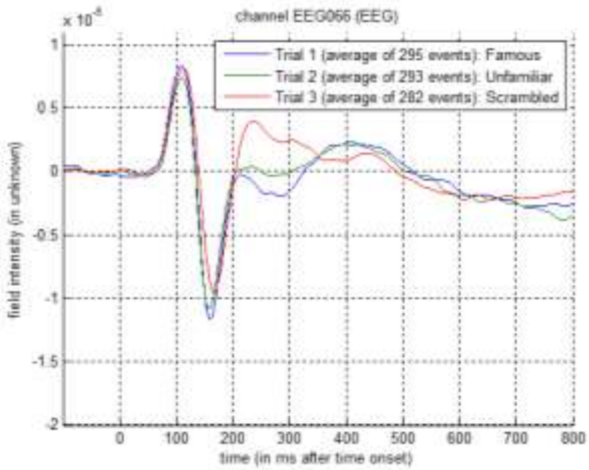


FIGURE 11. Subj # 3: channel # 66

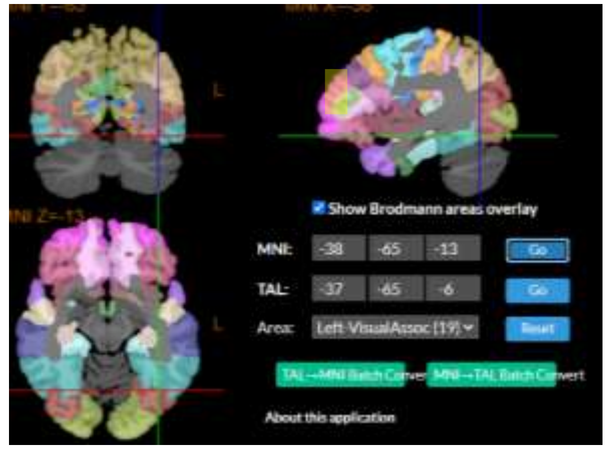


FIGURE 12. Subj # 1: EEG source localization

MSP inversion on using real EEG Dataset and fixed and varied patches from 256 - 350 provide different MNI coordinates as shown in Table I. These coordinates can be represented in the visual cortex. e.g. MNI coordinates for subj # 2 for fixed 256 patches are shown in Fig 12 [25]. However, as shown in Fig 13, some high active neural places are indicated by dark projections, whereas some light grey projects are also indicated in brain glass view. These light projections are called fake projections and are less active in the visual cortex. The neural responses achieved for subj # 1 are shown in Fig 14.

TABLE I
MNI COORDINATES FOR 3 X SUBJECTS

| MNI Coordinates with Fixed and Varied Patches | | | |
|---|---|---|---|
| Patches | Subj # 1 | Subj # 2 | Subj # 3 |
| 256 | [-38, -65, -13] | [50, -68, -8] | [41, -88, -8] |
| 350 | [-38, -65, -13] | [46, -79, 3] | [42, -64, 4] |
| 500 | [1, -25, 25] | [43, -68, -11] | [35, -82, 13] |
| 650 | [-43, -80, -12] | [44, -80, -15] | [46, -79, 3] |
| 800 | [-48, -69, -16] | [45, -81, -11] | [51, -68, 1] |
| 950 | [-48, -74, -15] | [42, -78, -4] | [42, -64, 4] |
| 1100 | [-38, -65, -13] | [40, -83, -14] | [47, -67, 3] |
| 1250 | [-49, -75, -8] | [48, -64 -13] | [-51, -68, 0] |
| 1400 | [-44, -74, -14] | [45, -81, -11] | [42, -64, 4] |
| 1550 | [-39, -61, -13] | [48, -77, 0] | [42, -64, 4] |
| 1700 | [-1, -35, 24] | [37, -69, -15] | [36, -20, -29] |
| 1850 | [-38, -65, -13] | [42, -78, -4] | [39, -81, -6] |
| 2000 | [-40, -65, -10] | [44, -80, -6] | [47, -67, 3] |
| 2150 | [-38, -65, -13] | [44, -80, -6] | [47, -67, 3] |
| 2300 | [43, -71, -15] | [45, -81, -11] | [-37, -24, -28] |
| 2450 | [-38, -65, -13] | [48, -64, -13] | [47, -67, 3] |
| 2600 | [1, -25, -25] | [44, -80, -6] | [56, -59, -16] |
| 2750 | [-40, -71, -16] | [54, -80, -15] | [50, -64, -2] |
| 2900 | [1, -25, 25] | [-44, -67, -13] | [35, -81, -3] |
| 3050 | [43, -71, -15] | [42, -78 -4] | [42, -78, -4] |
| 3200 | [-39, -61, -13] | [45, -81, -11 | [51, -68, 1] |
| 3350 | [-38, -71, -12] | [44, -80, -6] | [47, -67, 3] |
| 3500 | [-59, -39, -16] | [46, -79, 3] | [-46, -69, 5] |

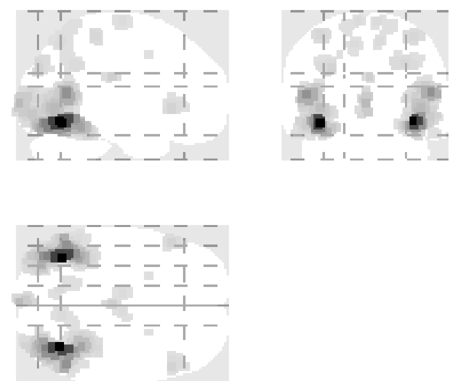

FIGURE 13. Subj # 1: Projections for fixed patches

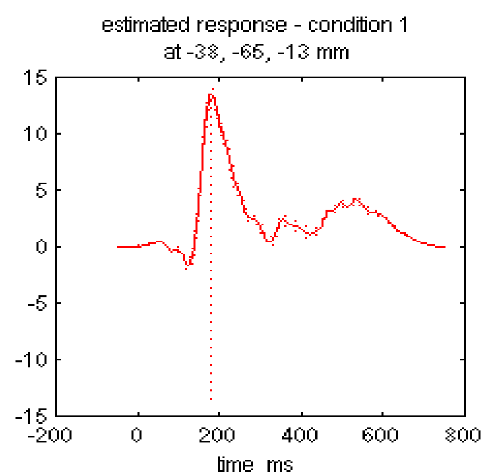


FIGURE 14. Subj # 1: Projections for fixed patches i.e. 256

However, FE computed from 3 x subjects is different due to experimental setup, head structures and ability to sight stimuli of grey images. Most of these neural sources are localized in fusiform and visual associative areas and their surroundings. The active neural projections at these MNI coordinates are shown in Fig 15 and Fig 16.

TABLE II
FREE ENERGY AND LOCALIZATION ERRORS OF 3 X SUBJECTS

| Patches | Subj # 1 | | Subj # 2 | | Subj # 3 | |
|---|---|---|---|---|---|---|
| Fixed// Varied | FE | Error [mm] | FE | Error [mm] | FE | Error [mm] |
| 256 | -1236.6 | Ref/. | -1236 | Ref. | -1029.8 | Ref. |
| 350 | -1239.4 | 7.73 | -1231.7 | 16.06 | -1022.9 | 26.85 |
| 500 | -1242.5 | 67.56 | -1234.2 | 7.62 | -1024.2 | 22.65 |
| 650 | -1235.7 | 15.84 | -1231 | 15.13 | -1022.3 | 15.07 |
| 800 | -1245.4 | 11.18 | -1238.7 | 14.25 | -1024 | 24.10 |
| 950 | -1237.4 | 13.60 | -1241.1 | 13.42 | -1020.8 | 26.85 |
| 1100 | -1233.2 | 15.89 | -1234.2 | 19.00 | -1023.4 | 24.45 |
| 1250 | -1237.4 | 15.68 | -1236.3 | 6.71 | -1021.9 | 94.49 |
| 1400 | -1239.8 | 10.86 | -1236.6 | 14.25 | -1020.8 | 26.85 |
| 1550 | -1235.3 | 4.12 | -1242.2 | 12.21 | -1020.8 | 26.85 |
| 1700 | -1234.4 | 60.37 | -1228.3 | 14.80 | -1020.5 | 71.34 |
| 1850 | -1241.8 | 65.56 | -1240.5 | 13.42 | -1025.6 | 7.55 |
| 2000 | -1235.8 | 3.60 | -1238.9 | 13.56 | -1017.9 | 24.45 |
| 2150 | -1236.3 | 5.123 | -1237.2 | 13.56 | -1020.3 | 24.45 |
| 2300 | -1239.2 | 81.25 | -1234.9 | 14.25 | -1019.9 | 102.86 |
| 2450 | -1235.4 | 59.32 | -1229.3 | 6.71 | 1019.2 | 24.45 |
| 2600 | -1232.8 | 57.14 | -1236.2 | 13.56 | -1023.7 | 33.61 |
| 2750 | -1234.7 | 7.01 | -1234.7 | 14.46 | -1024 | 26.32 |
| 2900 | -1231.8 | 67.56 | -1229.9 | 94.14 | -1026 | 10.49 |
| 3050 | -1232.9 | 81.25 | -1248.8 | 13.42 | -1027.8 | 10.82 |
| 3200 | -1234.5 | 4.12 | -1232.1 | 14.25 | -1023.5 | 24.10 |
| 3350 | -1238.6 | 6.08 | -1238.9 | 13.56 | -1018.8 | 24.45 |
| 3500 | -1235.2 | 33.56 | -1232.5 | 16.06 | -1023.5 | 89.99 |

As a result, it is demonstrated that most neural projections are explored in fusiform and associative areas of the brain's visual cortex, as shown by varying patches from 256 to 3500 Patches with a step size of 150 in Fig 15. However, these areas can be explored further by enhancing the number of patches with small step variations to achieve the optimized FE in the whole visual cortex of the brain. Thus, the proposed MSP patch variation algorithm provides the optimal FE with low localization error such as for Subj # 1, Optimal FE -1235.8 and fewer localization errors i.e. up to 3.6 mm is explored by varying the patches. The smooth desired results achieved are demonstrated in Fig 16.

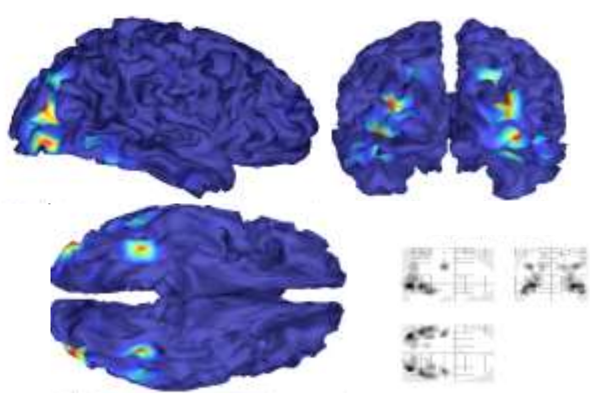

FIGURE 15. MSP Inversion (# 256 – 3500 patches)

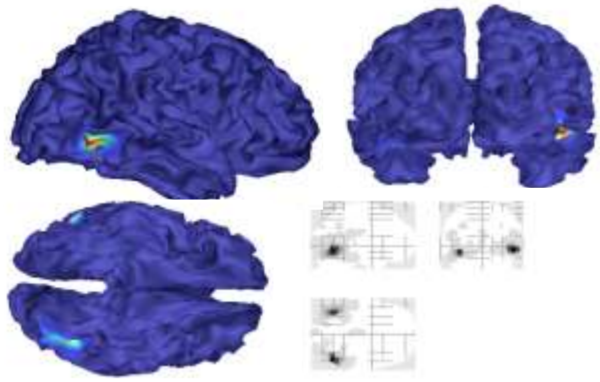

FIGURE. 16. MSP inversion giving optimized FE and low localization error

## VI. CONCLUSION

In this paper, the algorithm of MSP patches based Bayesian framework integrated with a synthetic EEG data generation scheme was developed and applied to optimize EEG source localization by varying the patches. EEG dataset of 3 x subjects (2 x Females, 1 x Male) with famous stimuli faces were selected. MSP inversion was run by using SPM12 Toolbox, where 23 x iterations varying patches from 256-3500 with an increment of 150 were individually run, and several desired optimal FE with low localization errors were achieved, as shown in Table II. MNI coordinate acquired from 256 patches was considered a reference point for ideal source localization. The same was validated through synthetic EEG generation, as shown in Figure 4, Fig 14 and Table I. It is also demonstrated that optimal FE was computed for a minimum localization error, i.e., 3.6 mm or even less, as shown in Table II. It is also analyzed that the most active neural areas for stimuli of famous faces are fusiform and associative areas of the visual lobe. Thus, it is concluded that optimal FE and minimum localization errors can be achieved only by using this proposed algorithm for visual applications and their source localizations in the human brain's visual cortex. This novel algorithm can be applied to improve visual neural sources and diagnose other brain diseases or disorders by placing electrodes on defective areas of the brain in the visual cortex.


## ACKNOWLEDGMENT

The authors are very thankful to Prof Richard Henson, Department of Psychiatry, MRC cognition and brain sciences unit, university of Cambridge, United Kingdom, for providing NOC and reference of the website for downloading and using the EEG dataset.

## FUNDING STATEMENT

The authors received no specific funding for this study.


## CONFLICTS OF INTEREST

The authors declare they have no conflicts of interest to report regarding the present study.

## REFERENCES


[1] A. Demertzi et al., "Human consciousness is supported by dynamic complex patterns of brain signal coordination," Science advances, vol. 5, no. 2, p. eaat7603, 2019.

[2] M. A. Lancaster et al., "Cerebral organoids model human brain development and microcephaly," Nature, vol. 501, no. 7467, p. 373, 2013.

[3] A. V. Apkarian, M. C. Bushnell, R. D. Treede, and J. K. Zubieta, "Human brain mechanisms of pain perception and regulation in health and disease," European journal of pain, vol. 9, no. 4, pp. 463-463, 2005.

[4] K. Rafik, B. H. Ahmed, F. Imed, and T.-A. Abdelmalik, "Recursive sLORETA-FOCUSS algorithm for EEG dipoles localization," in Image Processing Theory, Tools and Applications, 2008. IPTA 2008. First Workshops on, 2008, pp. 1-5: IEEE.

[5] C. Henderson, S. Butler, and A. Glass, "The localization of equivalent dipoles of EEG sources by the application of electrical field theory," Electroencephalography and clinical neurophysiology, vol. 39, no. 2, pp. 117-130, 1975.

[6] M. A. Jatoi, N. Kamel, A. S. Malik, I. Faye, and T. Begum, "A survey of methods used for source localization using EEG signals," Biomedical Signal Processing and Control, vol. 11, pp. 42-52, 2014.

[7] M. Heers, M. Helias, T. Hedrich, M. Dümpelmann, A. Schulze-Bonhage, and T. Ball, "Spectral bandwidth of interictal fast epileptic activity characterizes the seizure onset zone," NeuroImage: Clinical, vol. 17, pp. 865-872, 2018.

[8] A. Majkowski, Ł. Oskwarek, M. Kołodziej, and R. J. Rak, "An attempt to localize brain electrical activity sources using EEG with limited number of electrodes," Biocybernetics and Biomedical Engineering, vol. 36, no. 4, pp. 686-696, 2016.

[9] F. Costa, H. Batatia, T. Oberlin, and J.-Y. Tourneret, "Skull Conductivity Estimation for EEG Source Localization," IEEE Signal Processing Letters, vol. 24, no. 4, pp. 422-426, 2017.

[10] M. G. Stokes, M. J. Wolff, and E. Spaak, "Decoding rich spatial information with high temporal resolution," Trends in cognitive sciences, vol. 19, no. 11, pp. 636-638, 2015.

[11] M. R. Lakshmi, T. Prasad, and D. V. C. Prakash, "Survey on EEG signal processing methods," International Journal of Advanced Research in Computer Science and Software Engineering, vol. 4, no. 1, 2014.

[12] M. Gavaret, L. Maillard, and J. Jung, "High-resolution EEG (HR-EEG) and magnetoencephalography (MEG)," Neurophysiologie Clinique/Clinical Neurophysiology, vol. 45, no. 1, pp. 105-111, 2015.

[13] S. Vaid, P. Singh, and C. Kaur, "EEG signal analysis for BCI interface: A review," in 2015 Fifth International Conference on Advanced Computing & Communication Technologies, 2015, pp. 143-147: IEEE.

[14] A. T. Eggebrecht et al., "Mapping distributed brain function and networks with diffuse optical tomography," Nature photonics, vol. 8, no. 6, p. 448, 2014.

[15] C. J. Keller, C. J. Honey, P. Mégevand, L. Entz, I. Ulbert, and A. D. Mehta, "Mapping human brain networks with cortico-cortical evoked potentials," Philosophical Transactions of the Royal Society B: Biological Sciences, vol. 369, no. 1653, p. 20130528, 2014.

[16] M. Kalaivani, V. Kalaivani, and V. A. Devi, "Analysis of EEG signal for the detection of brain abnormalities," at International Journal of Computer Applications® year, 2014.

[17] V. Montes-Restrepo, P. van Mierlo, G. Strobbe, S. Staelens, S. Vandenberghe, and H. Hallez, "Influence of skull modeling approaches on EEG source localization," Brain topography, vol. 27, no. 1, pp. 95-111, 2014.

[18] J. Song et al., "EEG source localization: sensor density and head surface coverage," Journal of neuroscience methods, vol. 256, pp. 9-21, 2015.

[19] A. Sohrabpour, Y. Lu, P. Kankirawatana, J. Blount, H. Kim, and B. He, "Effect of EEG electrode number on epileptic source localization in pediatric patients," Clinical Neurophysiology, vol. 126, no. 3, pp. 472-480, 2015.

[20] G. F. Wu, R. Matthew, C. A.-L. Parks, B. M. Ances, and G. P. Van Stavern, "An eye on brain integrity: acute optic neuritis affects resting state functional connectivity," Investigative ophthalmology & visual science, vol. 56, no. 4, pp. 2541-2546, 2015.

[21] M. A. Jatoi, N. Kamel, J. D. López, I. Faye, and A. S. Malik, "MSP based source localization using EEG signals," in 2016 6th International Conference on Intelligent and Advanced Systems (ICIAS), 2016, pp. 1-5: IEEE.

[22] A. A. Gaho, S. H. A. Musavi, M. A. Jatoi, and M. Shafiq, "EEG Signals based Brain Source Localization Approaches," INTERNATIONAL JOURNAL OF ADVANCED COMPUTER SCIENCE AND APPLICATIONS, vol. 9, no. 9, pp. 253-261, 2018.

[23] M. A. Jatoi, N. Kamel, A. S. Malik, I. Faye, and T. Begum, "Representing EEG source localization using finite element method," in 2013 IEEE International Conference on Control System, Computing and Engineering, 2013, pp. 168-172: IEEE.

[24] A. A. Gaho, M. A. Jatoi, S. H. A. Musavi, and M. Shafiq, "Brain Mapping of Cortical Epileptogenic Zones and Their EEG Source Localization," in 2019 2nd International Conference on Computing, Mathematics and Engineering Technologies (iCoMET), 2019, pp. 1-6: IEEE.

[25] https://bioimagesuiteweb.github.io/webapp/mni2tal.html